Deep inelastic diffractive scattering with the ZEUS Forward Plug Calorimeter

Date : Apr. 23-27 2003

XI International Workshop on Deep Inelastic Scattering

Heuijin Lim (DESY) on behalf of the ZEUS Collaboration

- Introduction
- Measurement of diffractive cross section
  - Diffractive cross section
  - W dependence
  - $\alpha_{I\!P}(0)$
  - Ratio of diffractive to total cross section
  - Behaviour of $Q^2 d\sigma^{diff}_{\gamma^* p \to X N}/dM_X$ vs. M_X
- Measurement of diffractive structure function $F_2^{D(3)}(\beta, x_{I\!P}, Q^2)$
- Measurement of Pomeron structure function $F_2^{D(2)}(\beta, Q^2)$
- Summary

Inclusive Measurement of Diffraction in Deep Inelastic Scattering

- Measure the inclusive diffractive cross section
- Kinematics of $e + p \rightarrow e' + X + N$

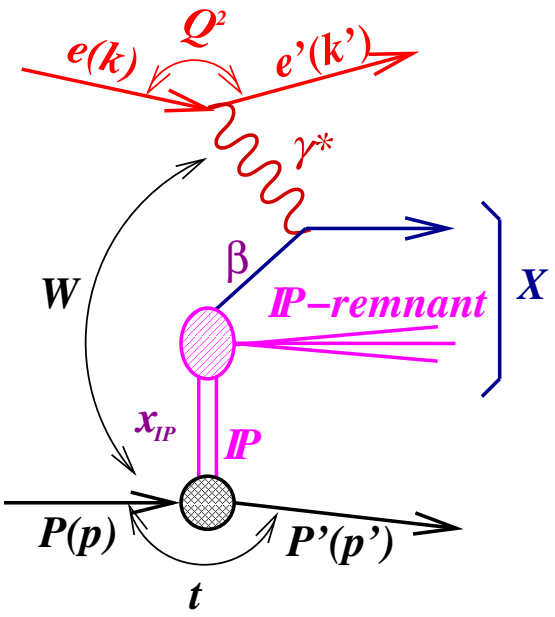

- $Q^2 = -q^2 = -(k - k')^2$
- $x = \dfrac{Q^2}{2q \cdot p}$
- $W = \sqrt{(p+q)^2}$
- $M_X^2 = (k - k' + p - p')^2$
- $x_{IP} = \dfrac{(p - p') \cdot q}{p \cdot q} \approx \dfrac{M_X^2 + Q^2}{W^2 + Q^2}$
- $\beta = \dfrac{Q^2}{2(p - p') \cdot q} = \dfrac{x}{x_{IP}} \approx \dfrac{Q^2}{M_X^2 + Q^2}$

- Analysis with $4.2\ pb^{-1}$ using $98/99$ data using ZEUS Forward Plug Calorimeter

	ZEUS 94	ZEUS 98-99
Q^2 (GeV^2)	7 - 140	2.2 - 80
W (GeV)	60 - 200	37 - 245
M_X (GeV)	$<$ 15	$<$ 35

M_X method using Forward Plug Calorimeter

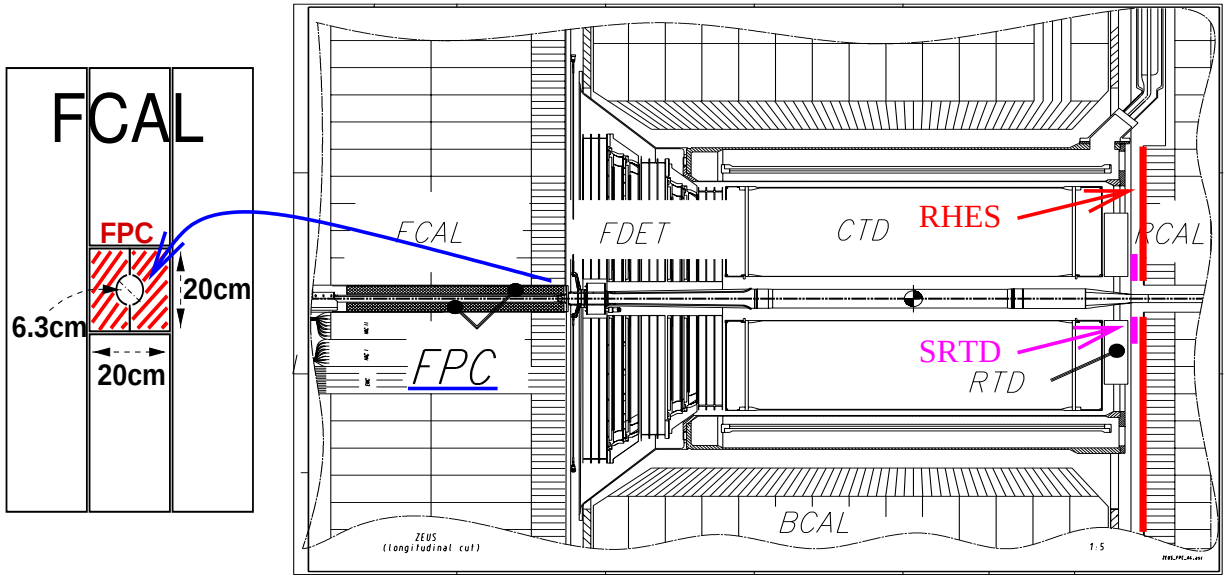

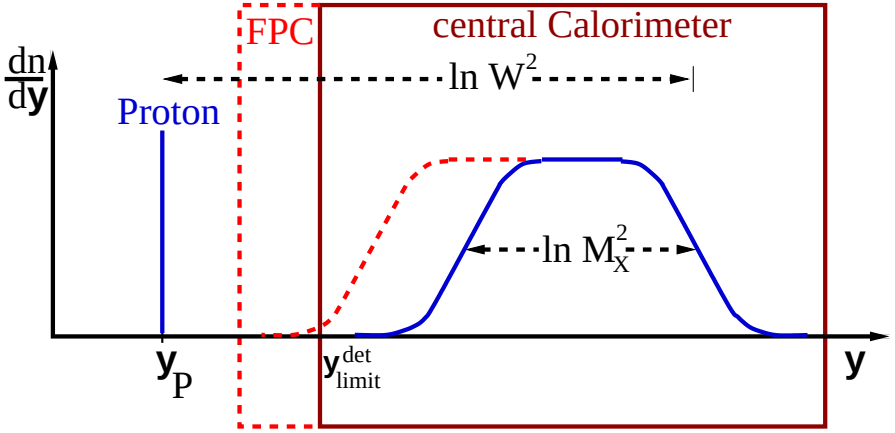

rapidity : $\mathcal{Y} = \frac{1}{2} \ln \frac{E + p_Z}{E - p_Z}$

pseudo-rapidity : $\eta = -\ln \tan(\frac{\theta}{2})$

with small mass ($E \simeq |p|$)

- Forward Plug Calorimter (FPC) : Shashlik type
  → Lead(1.5 cm)-Scintillator(0.26 cm)
  → N_{tot} of readout channel=60(EMC)+16(HAC)
- Extend calorimeter acceptance by 1 unit in pseudorapidity from η =4 to η =5.
  → Increase the accessible M_X range by a factor of 1.7
- For 1998-1999,
  - FPC → higher M_X and lower W
  - Smaller RCAL beamhole → lower Q^2 and higher W

Extraction of diffractive contribution

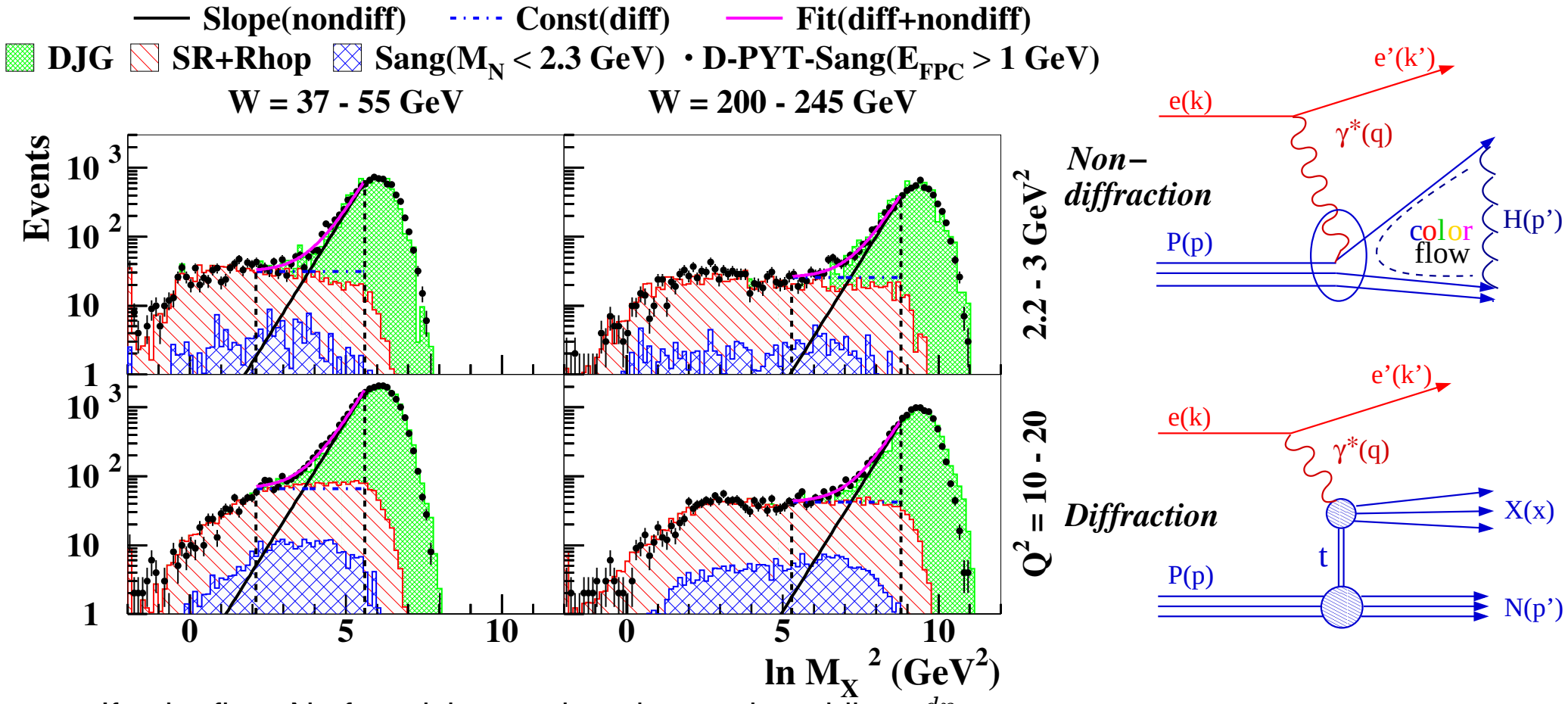

- If color flow, N of particles produced per unit rapidity : $\frac{dn}{d\mathcal{Y}} \approx \lambda \approx$ const
- $\frac{dN}{d\ln M_X^2} = D + c \cdot \exp(b \cdot \ln M_X^2)$ with free parameters, D , b and c from fit.

  $= \text{(Diff)} + \text{(Nondiff)}$
- We measure $d\sigma^{diff}_{\gamma^* p \to X N}/dM_X$, $M_N < 2.3$ GeV,

  if system N with $M_N \gtrsim 2.3$ GeV deposits $E_{FPC} > 1$ GeV. $\Longrightarrow$ Can recognize and reject!

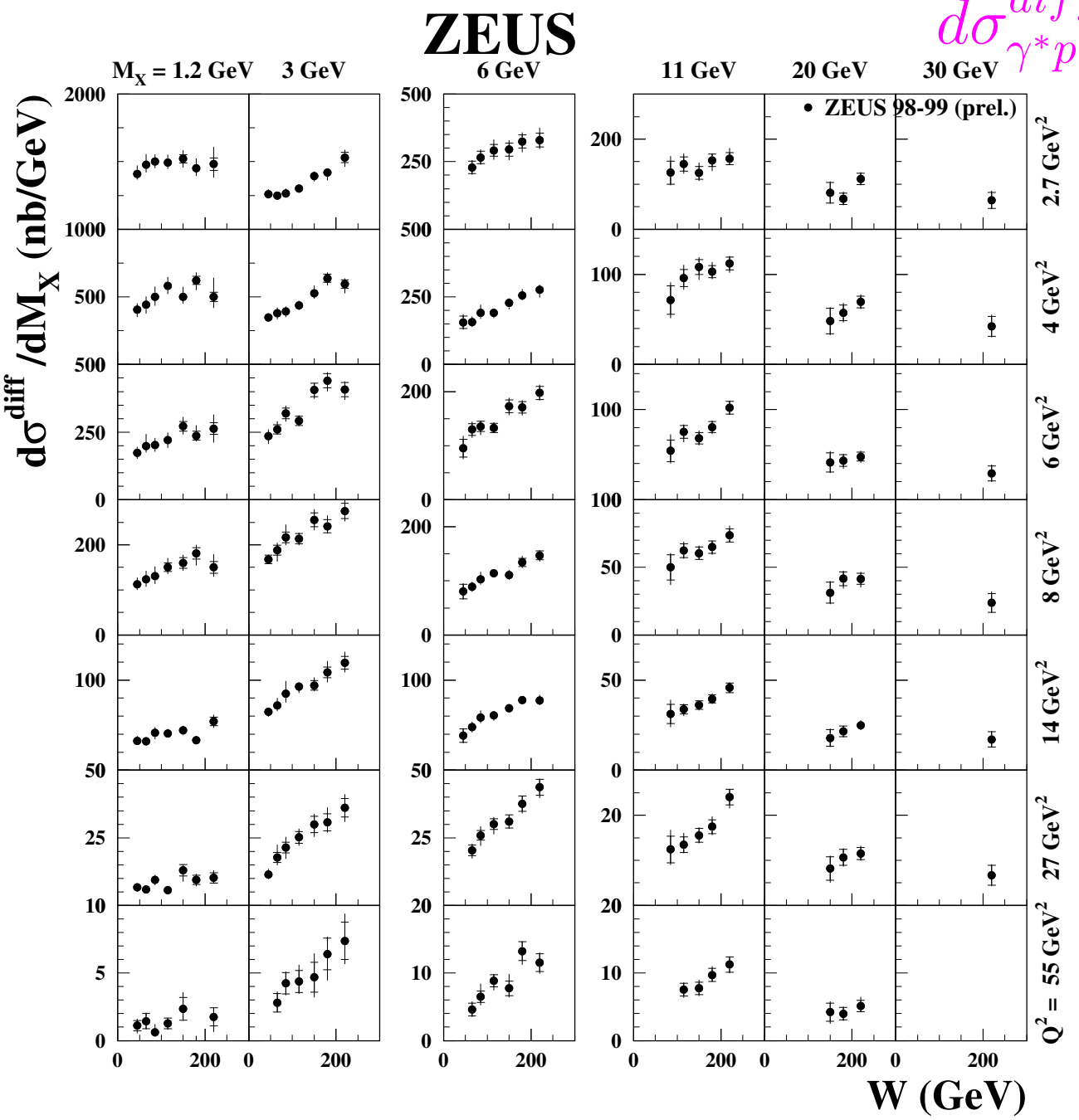

$$d\sigma^{diff}_{\gamma^* p \to X N}(M_X, W, Q^2)/dM_X,$$

$$M_N < 2.3 \text{ GeV}$$

- For $M_X < 2$ GeV, $d\sigma/dM_X$ depends weakly on W .
- For $M_X > 2$ GeV, $d\sigma/dM_X$ rises rapidly with W.

W dependence of $d\sigma^{diff}_{\gamma^* p \to X N}/dM_X$

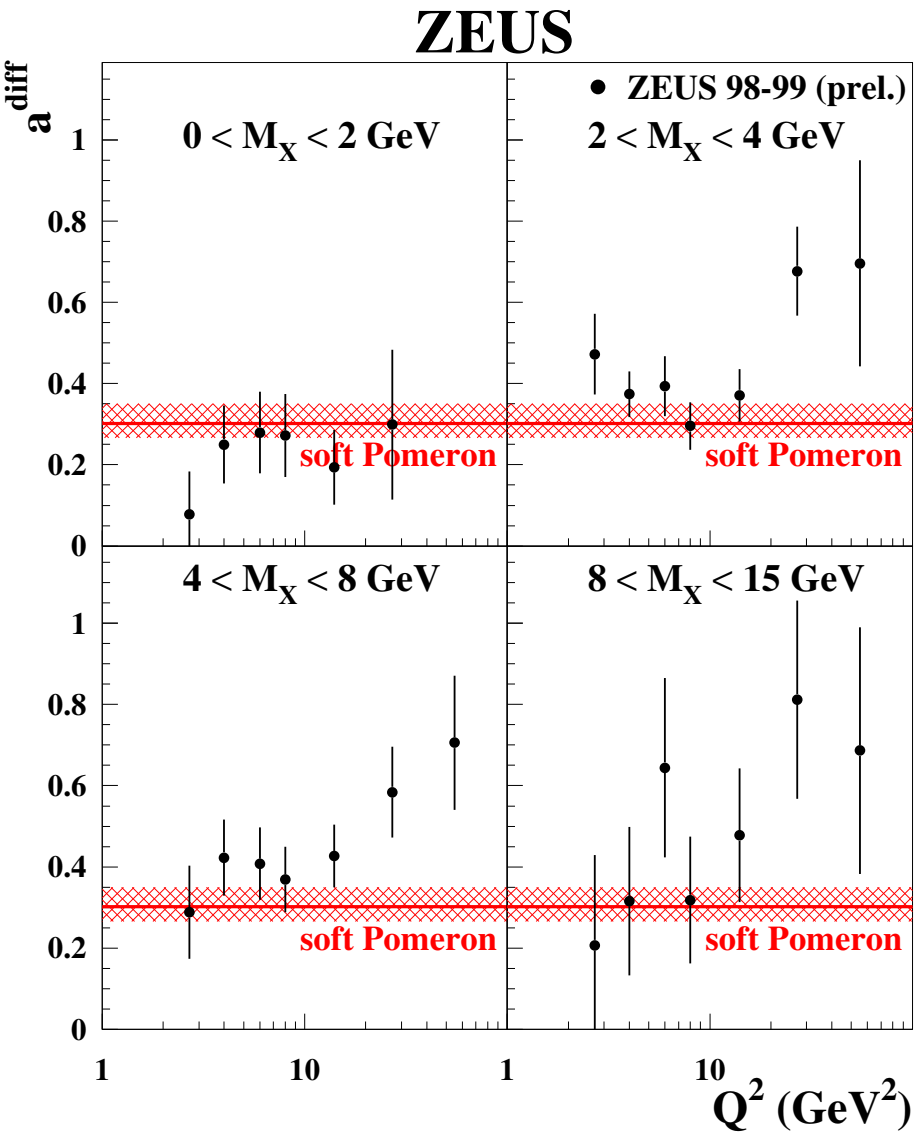

1. Fit

$$\frac{d\sigma^{diff}_{\gamma^* p \to X N}}{dM_X} = h \cdot W^{a^{diff}} \sim (W^2)^{(2\overline{\alpha_{IP}}-2)}$$

(h , a^{diff} free parameters)

$\therefore \overline{\alpha_{IP}} = 1 + a^{diff}/4$

2. Compare with soft pomeron,

$\alpha^{soft}_{IP}(0) = 1.096^{+0.012}_{-0.009}$

(from hadron-hadron scattering at $t = 0$)

$\therefore a^{soft} = 0.302^{+0.048}_{-0.036}$

(corrected by 0.02($= \delta\alpha_t$) for t distribution)

3. For $M_X < 2$ GeV, a^{diff} is like for the soft pomeron.

4. At higher M_X , a^{diff} is higher than expected from the soft pomeron and increases with Q^2 .

$\Longrightarrow$ Above soft pomeron!

Note : For $Q^2 > 10$ GeV^2 ,

Probability that $a^{diff} = a^{soft}$ is < 0.001

$\Longrightarrow$ Strong indication for pQCD

Compare α_{IP} for diffractive and total $\gamma^* p$ scattering

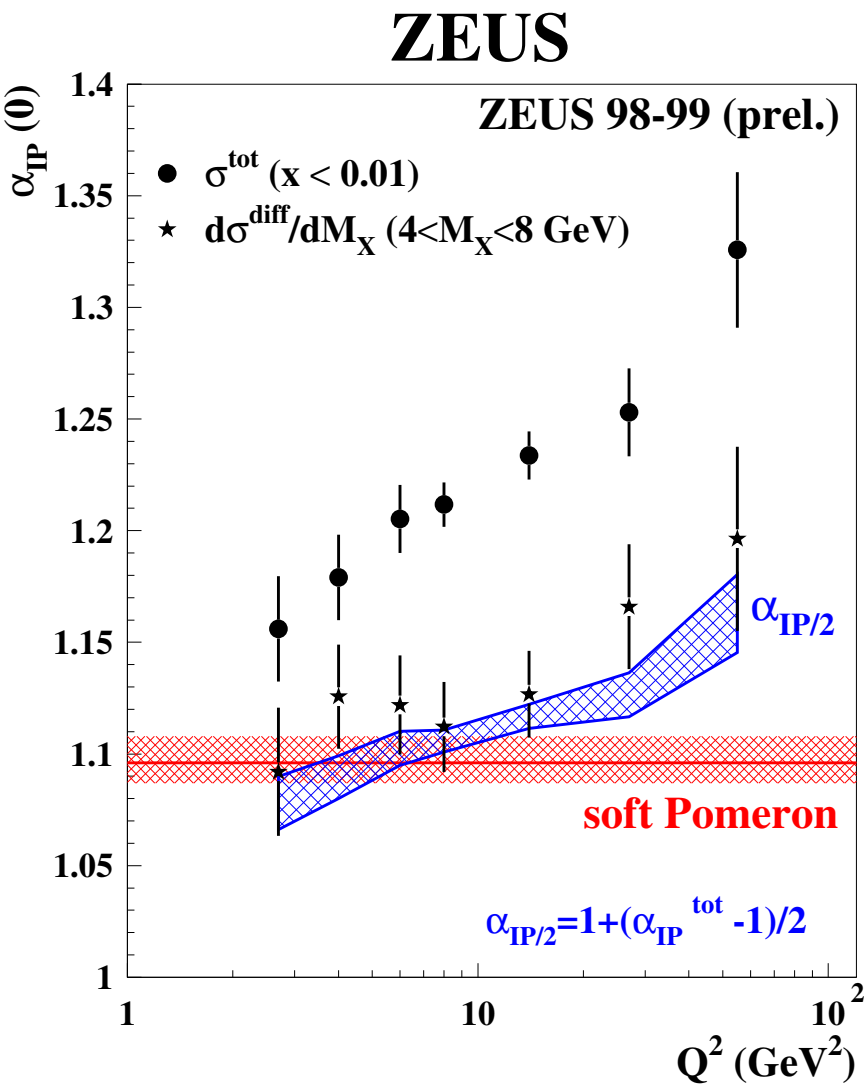

- $\sigma^{tot}_{\gamma^* p} = \dfrac{4\pi^2\alpha}{Q^2} \cdot F_2(x, Q^2)$

  $\sim \dfrac{1}{W^2} ImT_{\gamma^* p \to \gamma^* p}(W^2, t=0) \sim (W^2)^{\alpha^{tot}_{IP}(0)-1}$

  (Optical theorem)

- $\dfrac{d^2\sigma^{diff}}{dM_X dt} \sim \quad |T_{\gamma^* p \to \gamma^* p}|^2 \quad \sim (W^2)^{2(\alpha^{diff}_{IP}(0)-1)}$

  at $t = 0$

- Data ($4 < M_X < 8$ GeV) show

  $\Longrightarrow \alpha^{diff}_{IP} \approx 1 + (\alpha^{tot}_{IP} - 1)/2$

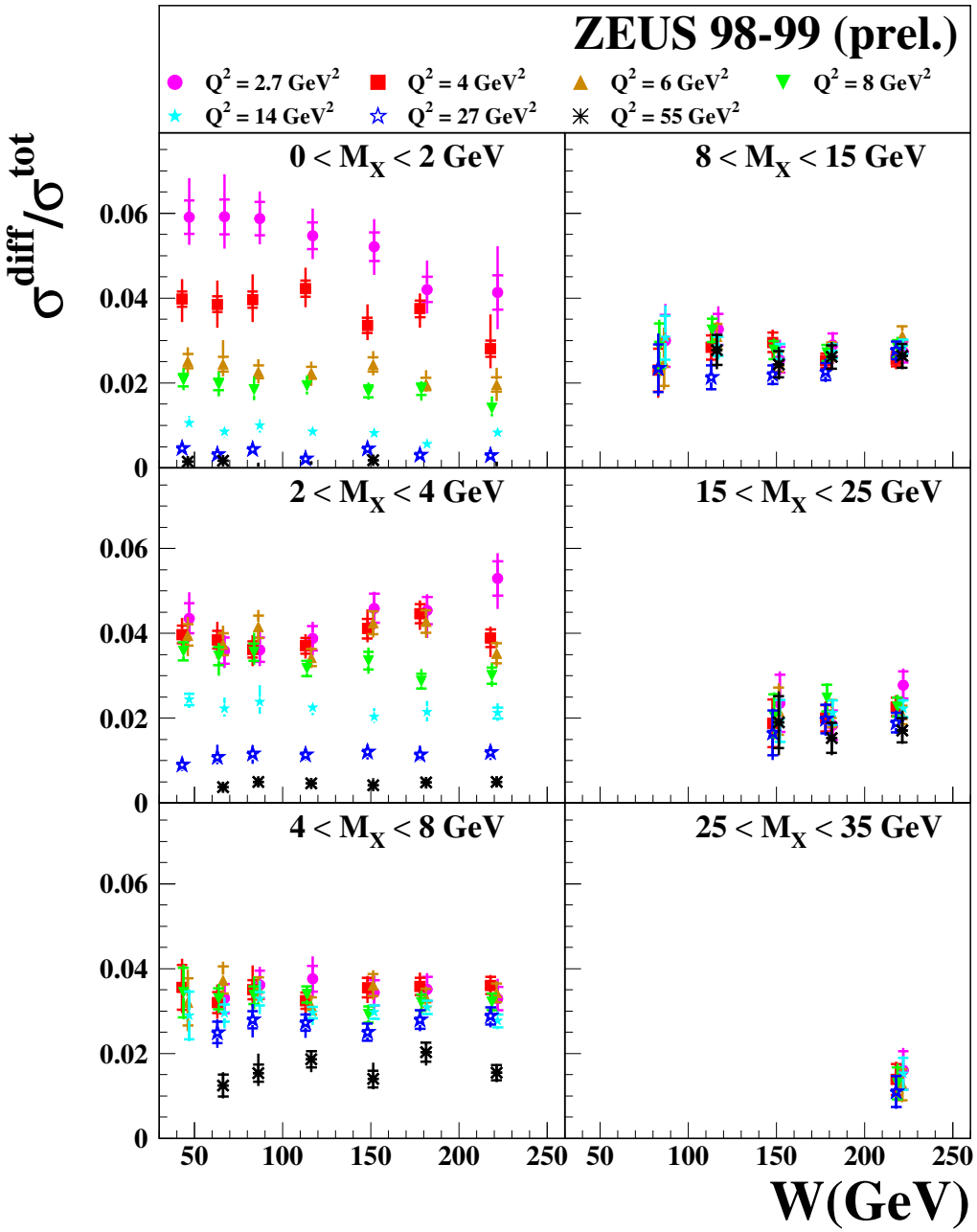

$$r_{tot}^{diff} = \frac{\int_{M_a}^{M_b} dM_X d\sigma_{\gamma^* p \to X N, M_N < 2.3 GeV}^{diff} / dM_X}{\sigma_{\gamma^* p}^{tot}}$$

- For $M_X < 2$ GeV, r_{tot}^{diff} is falling with W .
- For $M_X > 2$ GeV, r_{tot}^{diff} is constant with W .
  $\Longrightarrow$ The diffractive cross section has about the same W -dependence as σ^{tot} .
- The low M_X bins exhibit a strong decrease of r_{tot}^{diff} with increasing Q^2 .
- For $M_X > 8$ GeV, no Q^2 dependence is observed.
- At $W = 220$ GeV,
  $\sigma_{(M_X < 35 \text{ GeV})}^{diff} / \sigma^{tot} \sim 20\%$ at $Q^2 = 2.7$ GeV^2
  $\sim 10\%$ at $Q^2 = 27$ GeV^2
  $\Longrightarrow$ Slowly decreasing with Q^2

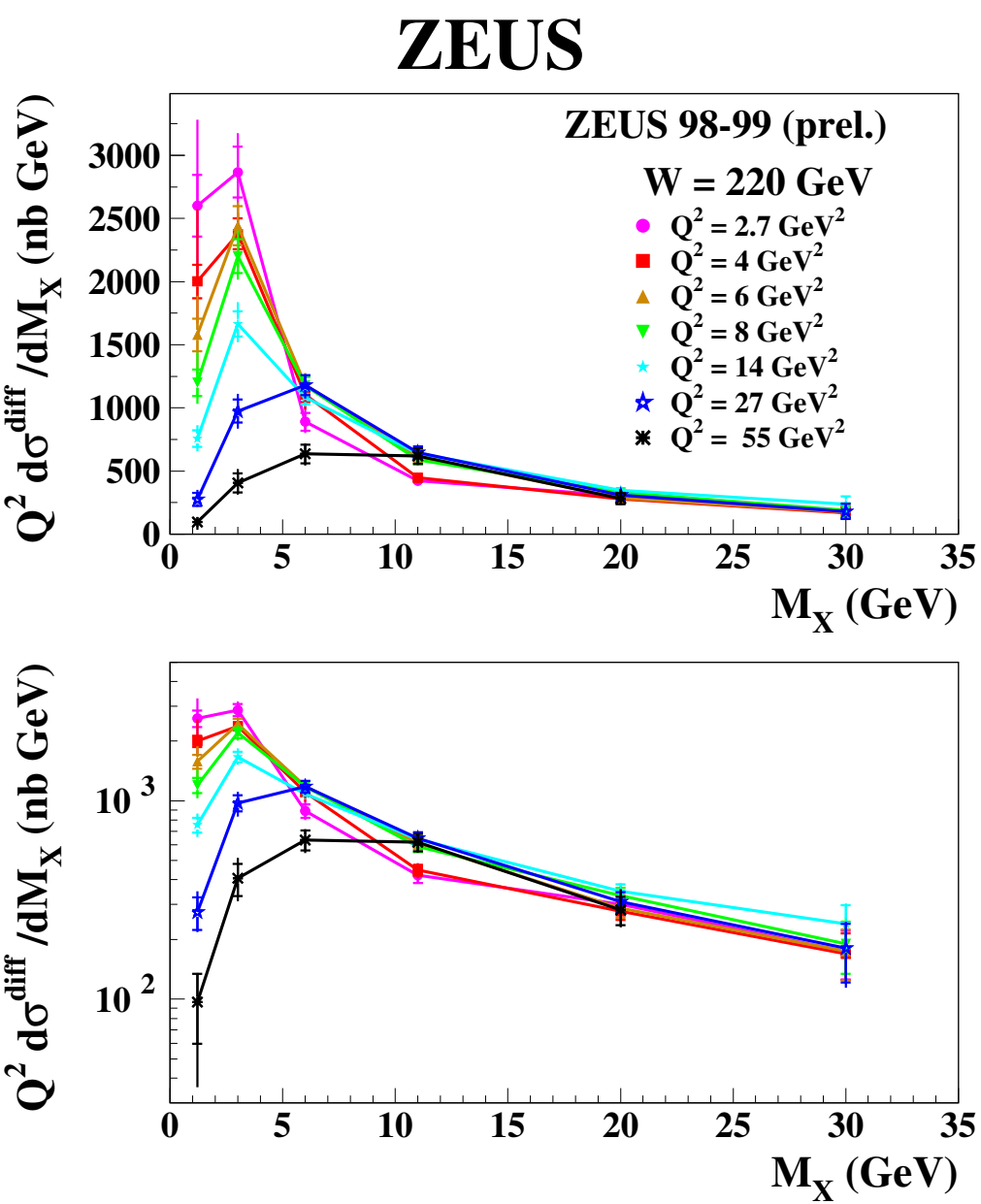

$Q^2 d\sigma^{diff}_{\gamma^* p \to X N}/dM_X$ vs. M_X at $W = 220$ GeV

- Rapid decrease with Q^2 for $M_X < 4$ GeV
  $\Longrightarrow$ predominantly higher twist.
- Constant or slow rise with Q^2 for $M_X > 10$ GeV
  $\Longrightarrow$ leading twist.

Diffractive structure function $F_2^{D(3)}$

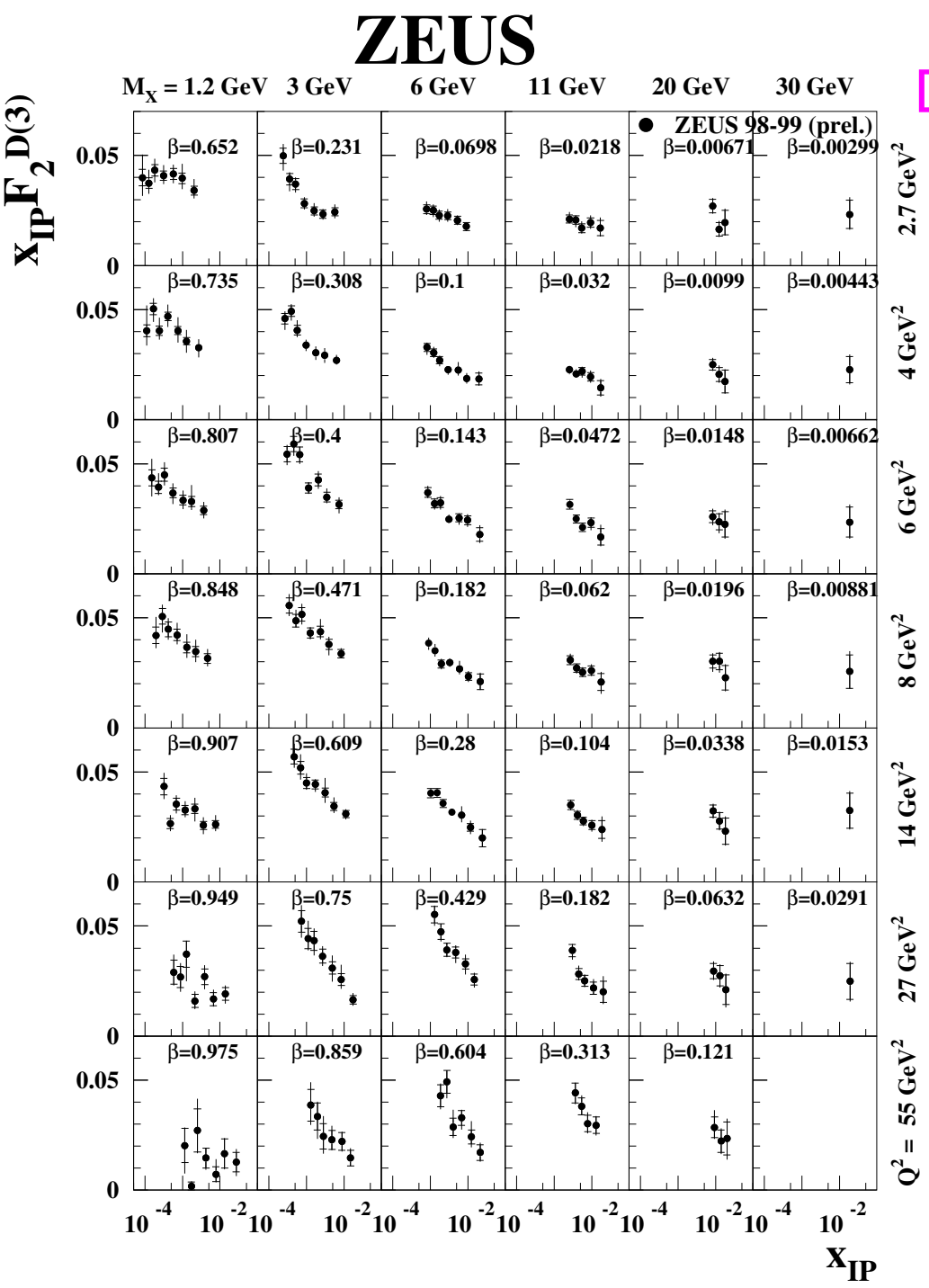

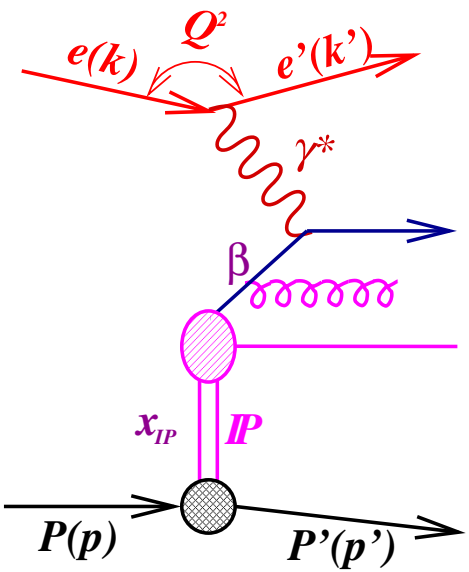

- $x_{IP}F_2^{D(3)}(\beta, x_{IP}, Q^2) = \frac{1}{4\pi^2\alpha} \cdot \frac{Q^2(Q^2+M_X^2)}{2M_X} \cdot \frac{d\sigma^{diff}_{\gamma^* p \to XN}}{dM_X}$
- $M_X < 2$ GeV, $x_{IP}F_2^{D(3)}$ is constant with x_{IP} .
- $M_X > 2$ GeV, rapid increase as $x_{IP} \to 0$.

  i.e. parton evolution as $x_{IP} \to 0$.

Comparison with the BEKW model

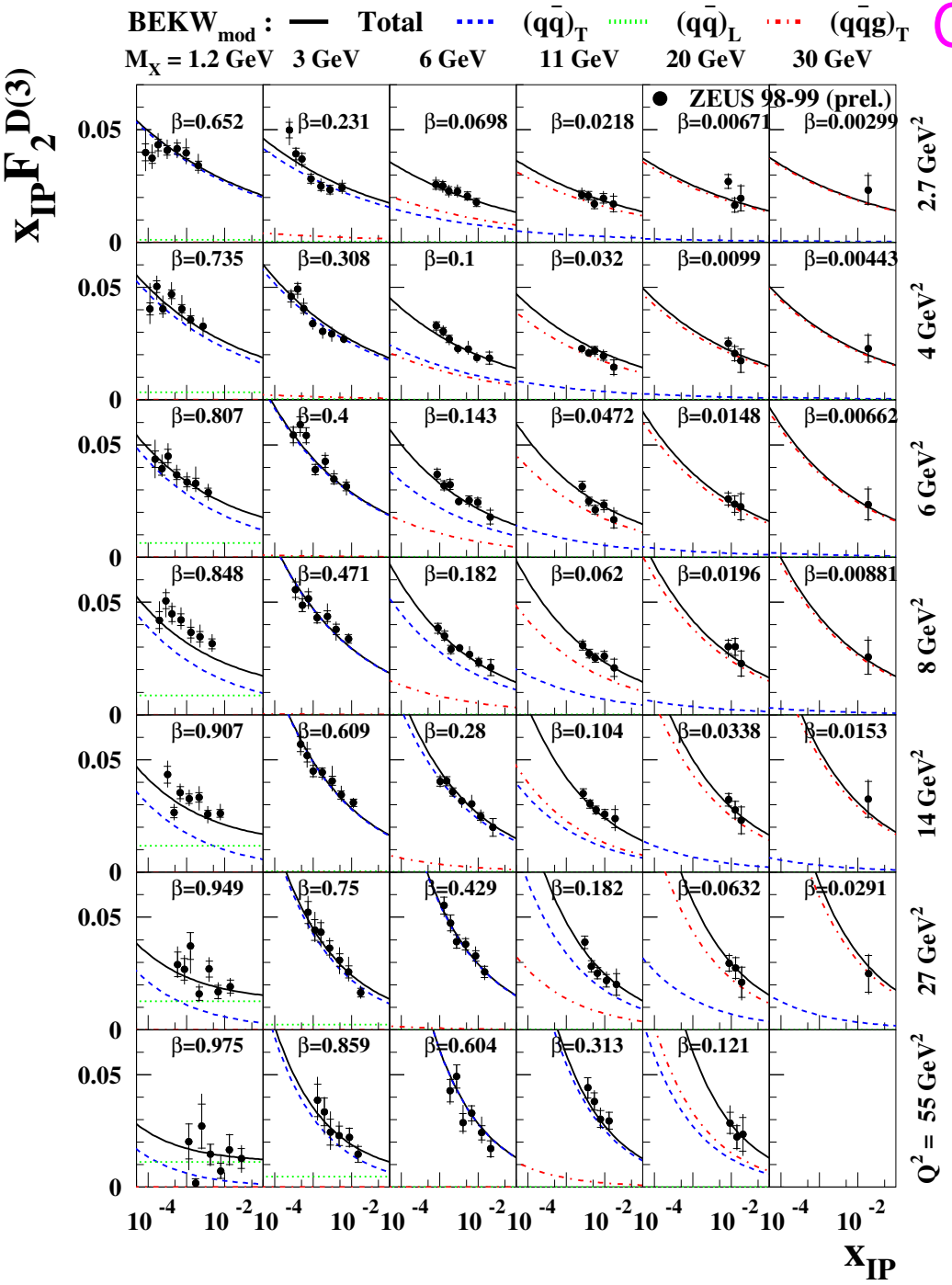

(Bartels, Ellis, Kowalski and Wüsthoff, 1998)

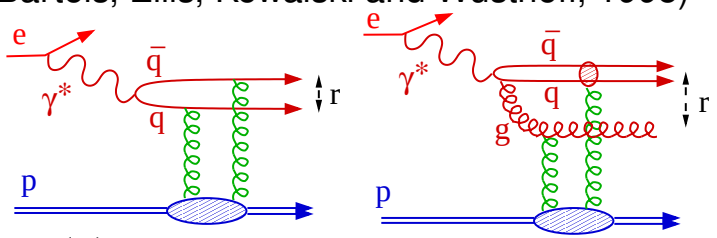

- $x_{IP}F_2^{D(3)} = c_T \cdot F_{q\bar{q}}^T + c_L \cdot F_{q\bar{q}}^L + c_g \cdot F_{q\bar{q}g}^T$

$$F_{q\bar{q}}^T = (\frac{x_0}{x_{IP}})^{n_T(Q^2)} \cdot \beta(1-\beta)\,,$$

$$F_{q\bar{q}}^L = (\frac{x_0}{x_{IP}})^{n_L(Q^2)} \cdot \frac{Q_0^2}{Q^2} \cdot [\ln(\frac{7}{4} + \frac{Q^2}{4\beta Q_0^2})]^2 \cdot \beta^3(1-2\beta)^2\,,$$

$$F_{q\bar{q}g}^T = (\frac{x_0}{x_{IP}})^{n_g(Q^2)} \cdot \ln(1+\frac{Q^2}{Q_0^2}) \cdot (1-\beta)^\gamma$$

From data, $n_L(Q^2) \approx 0$ and

$$n_T(Q^2) \approx n_g(Q^2) \approx n_1 \ln(\frac{Q^2}{Q_0^2})$$

$\therefore c_T = 0.118 \pm 0.027, c_L = 0.141 \pm 0.011$

$c_g = 0.0093 \pm 0.0003, n_1 = 0.068 \pm 0.0032$

$\gamma = 8.48 \pm 0.51, \chi^2/\text{ndf} = 175/(204-5)$

- While the $(q\bar{q})_L$ contribution decreases rapidly as M_X increases, $(q\bar{q})_T$ and $(q\bar{q}g)_T$ increase with M_X . $(q\bar{q}g)_T$ dominates at high M_X .

Pomeron structure function $F_2^{D(2)}(\beta, Q^2)$

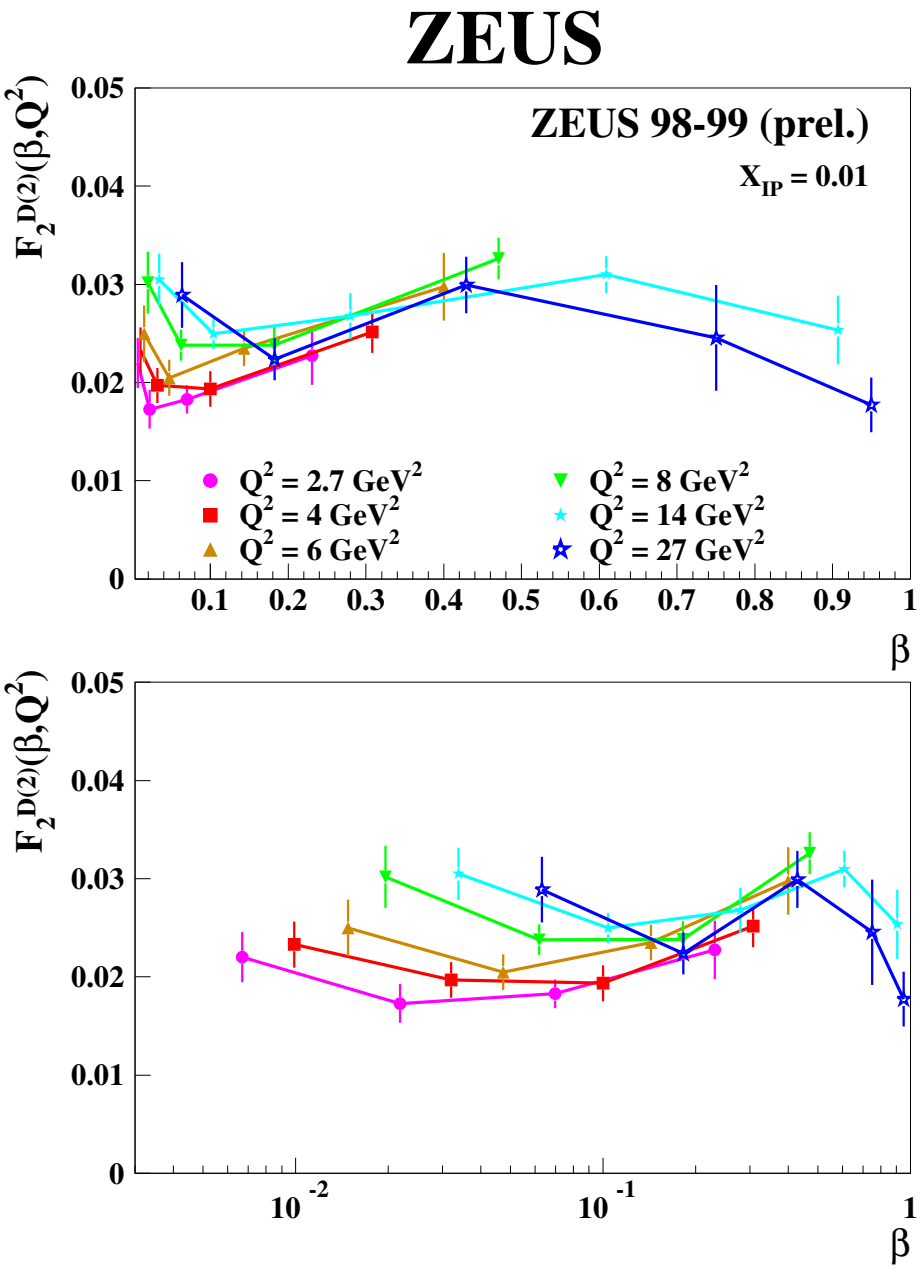

- Structure Function, Proton $x, Q^2 \rightarrow F_2(x, Q^2)$

  Pomeron $\beta, Q^2 \rightarrow F_2^{D(2)}(\beta, Q^2)$

  $\Longrightarrow$ Probability to find a quark with momentum fraction β in the Pomeron

- Following the BEKW model,

  $F_2^{D(3)}(Q^2, \beta, x_{IP}) = f_{IP/p}(x_{IP}, Q^2) \cdot F_2^{D(2)}(\beta, Q^2)$

  Here, $f_{IP/p}(x_{IP}, Q^2)$ is the Pomeron flux factor.

  use ansatz $f_{IP/p}(x_{IP}, Q^2) = \dfrac{C}{x_{IP}} \cdot (\dfrac{x_0}{x_{IP}})^{n(Q^2)}$.

- We set $x_0 = 0.01$, $C = 1$

  $\Longrightarrow$ determine $F_2^{D(2)}$ at $x_{IP} = 0.01$

  $\therefore F_2^{D(2)}(\beta, Q^2) = x_0 F_2^{D(3)}(x_0, \beta, Q^2)$

- For high β , $F_2^{D(2)}$ decreases with rising Q^2 .

- As $\beta \rightarrow 0$, $F_2^{D(2)}$ rises. The rise becomes more strong as Q^2 increases.

  $\Longrightarrow$ Evidence for pQCD evolution

Summary

	$M_X < 2$ GeV	$M_X > 2$ GeV
$d\sigma^{diff}/dM_X$	Constant with W	Rising with W
$\alpha_{I\!P}(0)$	like soft pomeron	For $Q^2 > 10$ GeV^2 , above soft pomeron and rising with Q^2
r_{tot}^{diff}	Falling with W Decreasing with Q^2 for $M_X < 8$ GeV	Constant with W Weak Q^2 dependence for $M_X > 8$ GeV
$Q^2 d\sigma^{diff}/dM_X$	Decreasing with Q^2 $\Longrightarrow$ Higher twist	Constant for $M_X > 10$ GeV $\Longrightarrow$ Leading twist
$x_{I\!P} F_2^{D(3)}$	Constant w.r.t. $x_{I\!P}$	Rising as $x_{I\!P} \to 0$
	"valence region", $\beta > 0.1$	"sea region", $\beta < 0.1$
$F_2^{D(2)}(\beta, Q^2)$	Decreasing with Q^2 Maximum at $\beta \sim 0.5$, $I\!P = q\bar{q}$	Increasing as $\beta \to 0$ Increasing with Q^2

$\Longrightarrow$ DIS diffractive Scattering : Evidence for QCD evolution in $x_{I\!P}$ and in β.